A Highly Sensitive Dual-Band RF Glucose Sensor with Diamagnetic Metasurface Transitions

Sudershan Dutt[a], Louis WY Liu[b***], Pawan Kumar[a], Ali M. Almuhlafi[c], Hamsakutty Vettikalladi[c], Tobore Igbe[d], Endalkachew Girma Andargie[e*], Abhishek Kandwal[f**]

[a]School of Physics and Materials Science, Shoolini University, H.P, India
[b]Faculty of Engineering, Vietnamese German University, Vietnam
[c]Electrical Engineering Department, King Saud University, Riyadh, Saudi Arabia
[d]School of Computing and Digital Technology, Redeemer's University, Ede, Osun Sate, Nigeria
[e]Armauer Hansen Research Institute, Adis Ababa, Ethiopia
[f]School of CHIPS, Xian Jiaotong-Liverpool University, Suzhou, China

Corresponding emails: endalkachew.girma@ephi.gov.et *, abhishekandwal@gmail.com **and liu.waiyip@vgu.edu.vn ***

Abstract

For microwave glucose sensing without a vector network analyzer (VNA), one of the options is to measure the reflection coefficient of a glucose sensor using a gain-phase detector. Gain-phase detectors have a frequency threshold, and, in the case of AD8302, the threshold frequency is 2.7 GHz. In this work, focus has been placed on realizing a glucose sensing device compatible with AD8302. Methodology: A sensing device with two resonant frequencies below the threshold frequency of AD8302 was realized on a lossy FR4 substrate in a way to allow the measurements to be cross-checked within a narrow frequency range. The realized sensor features the use of two closely packed periodic arrays of closed metal rings in the energy transfer region. On the other hand, a near-Littrow configuration was successfully used in the sensing region for detection of ultra-low concentration of glucose in a liquid solution. The fabricated sensor has exhibited dual resonances, with one resonance occurring at around 2.42 GHz and the other occurring at around 1.65 GHz. The minimum detectable glucose concentration of the proposed glucose sensor was found to be 25 mg/dL. The sensitivities that have been achieved were 715 kHz/(mg/dL) at around 2.42 GHz, and 805 kHz/(mg/dL) at around 1.65 GHz. Overall, a glucose sensing device with a dual resonant frequency characteristic has been realized with a minimum detectable glucose concentration at 25 mg/dL and a maximum sensitivity at 805 kHz/(mg/dL).

Keywords: Glucose; RF; Microwave; Instrumentation; Measurement; Sensor; Diamagnetism; AD8302; Gain-phase detector;

I. Introduction

The history of minimally invasive glucose sensing started at around 2009. Back in 2009, the world witnessed major advancements in glucose sensing, with Dexcom and Abbott introducing their real-time Continuous Glucose Monitors (CGMs) to the global diabetic community. The CGMs from Dexcom and Abbott are not qualified as non-invasive sensors because these devices still require a small glucose sensor to be inserted under the skin to operate. Unlike the traditional invasive lancet techniques, however, CGMs were minimally invasive and offered real-time tracking of meals/insulin, thereby improving blood glucose control in Type 1 diabetic population. For the first time in human history, these products marked a transition from the traditional finger-prick method towards computerized CGM systems that has been proven helpful for the diabetic community [18].

However, being a minimally invasive sensors, real-time CGMs have not significantly stirred up any serious research interest in the global scientific community. Figure 1 shows the number of IEEE journal papers that were published per year and that were categorized as glucose related by the search engine in Ieeexplore. According to the data from IEEE, the number of yearly published journal papers in the field of glucose sensing were no more than 100 from 2011 to 2020, suggesting that the global research productivity in glucose sensing used to be very stagnant before 2020. The lack of research interests in glucose sensing before 2020 was in part attributed to the shortage of societal needs, and in part attributed to the shortage of resources for this research.

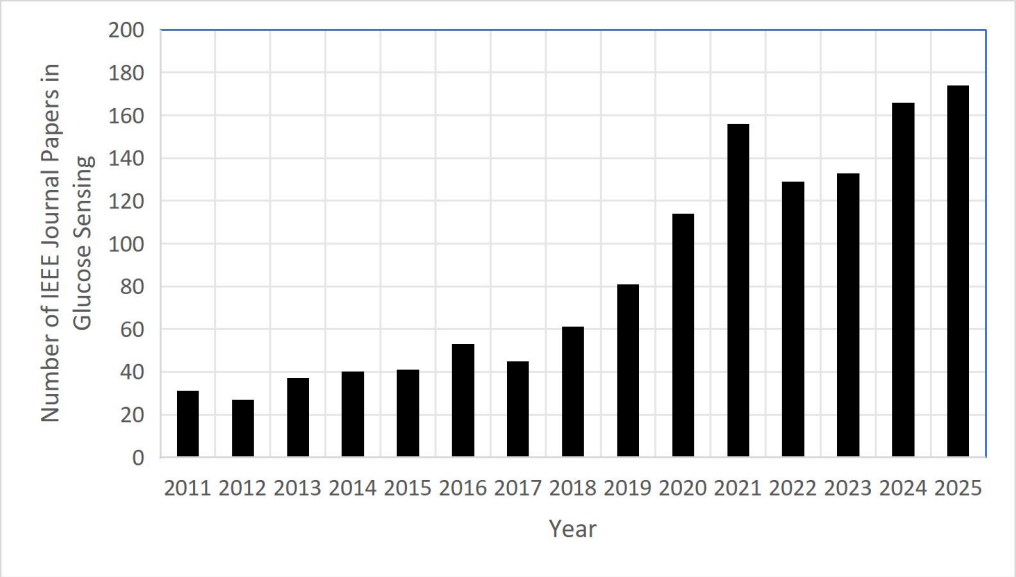

Figure 1. Number of IEEE Journal Papers in Glucose Sensing Per Year

Due to the outbreak of COVID-19, however, the research into glucose sensing started to receive attention from the scientific community in 2019. During the year of 2021, the world experienced an unprecedented lockdown, whilst the number of IEEE journal papers related to glucose sensing noticeably spiked up to 156. Unlike the decade before 2020, the number of journal papers from

IEEE have been steadily increasing with no sign of stopping. There is no suggestion that the field of glucose sensing is running of the research. Up until now, the majority of published investigations mainly focused on non-invasive sensing via electromagnetic (EM) perturbation that uses the interaction between EM waves (typically microwaves or radio frequency waves) and glucose loaded sample to estimate the blood glucose concentration. This method leverages the principle that glucose concentration changes the dielectric properties (permittivity) of a medium but, up until now, most of the published experimental sensors have to operate in conjunction with a vector network analyzer. In these investigations, however, the frequencies of operation of the sensors were apparently not the major primary concern. On the other hand, vector network analyzers (VNA) are not only expensive but also difficult to customize using microcontrollers. VNA's are not something that can be afforded by an average individual from a diabetic population.

Nowadays, glucose sensing is becoming mainstream research in the global research community, in part because of the recent global outbreak of coronavirus pandemics, and in part because of the availability of devices capable of conducting highly complicated analog computation. These devices are often considered to be cheaper, but more flexible, alternative to VNA. Examples of these devices are the well-known gain phase detector from Analog Devices, AD8302. Unlike the old days, many highly complicated tasks have been accomplished with the help of the gain phase detectors. The work from Liu [2] and Pockevicius [3] were among these examples. However, the use of AD8302 in the field of glucose sensing is currently still very rare. In Gelao's work [1], for example, a waveform generator (AD9954) together with a gain-phase detector (AD8302) were used to implement an impedance measuring device working in a frequency range of 1MHz-160MHz. The main problem of those gain-phase detectors is that most of these products have a very low frequency threshold. In AD8302, for example, the maximum operating frequency is 2.7GHz. Regrettably, most of the experimental electromagnetic glucose sensors of this date resonate at much higher frequencies. The examples listed in Table 1 are the exception.

Table 1: Electromagnetic Glucose Sensors that can straightforwardly operate in conjunction with AD8302

Reference	Topology	Operating Frequencies (GHz)	Sensitivity (MHz/mg/dL and/or dB /mg/mL)	Sensor Size
5	Double Split-ring Resonator	1.7, 4.4	24 MHz/mg/dL	35 × 50 mm^2
6	Complementary SRR	2.4	Not reported	20 × 34 mm^2
7	Coupling Resonant Circuit involving an antenna, mixer	1.6	Not reported	~70 × 70 mm^2

	and RSSI			
8	Bifilar Resonator	0.640	130 MHz/mg/mL & 4 dB /mg/mL	20 × 10 mm^2
9	Microstrip U-shape resonator	0-1	0.150 MHz/(mg/dL)	37 × 20 mm^2
This work	A near-Littrow configuration together with a periodic array of closed circular metal rings.	2.38-2.48 GHz and 1.61-168 GHz	0.715 MHz/(mg/dL) at the 2.42 GHz, and 0.805 MHz/(mg/dL) at 1.54 GHz	40 × 150 mm^2

For a glucose sensor to be able to operate with any of the commercially available gain-phase detectors, the resonant frequency of the sensing head should not exceed the threshold frequencies of the gain-phase detectors. It was for this reason why the primary objective of this work was realization of a glucose sensing device with resonant frequencies below the frequency threshold of the commercially available gain-phase detector (e.g. AD8302), typically and preferably less than 2.7 GHz.

In addition to fulfilling the main objective of this work, the following novelties have been achieved:

1) The design of the realized sensor was primarily based on two closely packed periodic arrays of closed metal rings.

2) A near-Littrow configuration has been successfully used in the sensing region for detection of ultra low concentration of glucose in a liquid solution, with the minimum concentration down to 0 mg/dL.

3) The sensitivities that have been achieved were 0.715 MHz/(mg/dL) at the primary resonance, and 0.805 MHz/(mg/dL) at the secondary resonance.

4) The proposed glucose sensor was found to be resonate at two different frequencies within a narrow frequency range, thereby allowing the measurements to be cross-checked with minimal hardware resources.

II. Methodology

Figure 2 depicts the details of the proposed glucose sensor. Figure 2a shows the electron scanned image of the proposed sensor that has been photo-lithographically. The proposed sensor

comprises three distinct regions, namely the transition and tapered region, the energy transfer region and the sensing region.

As shown in Figure 2d, the results of CST simulation and measurement suggests the proposed sensor should be able to exhibit two independent resonances, with the primary resonance was achievable at 2.5GHz and with the other at 1.66 GHz. The resonance at 1.66 GHz was believed to be caused by the plasmonic resonance due to the reflection from the near Littrow configuration. Due to the negative interference caused by the glucose water molecules on the near-Littrow configuration, the Q-factor for the resonance at 1.66 GHz was expected to be lower than the simulated results.

In the sections which follows, the tapered region, the energy transfer region and the sensing region are individually discussed along with a discussion on sensitivity as well as the experimental setup.

(b)

(c) (d)

Figure 2. Details of the Proposed Sensor. (a) The electron scanned image; (b) The simulated electric field at 2.5 GHz; (c) The simulated far field, and (d) S-parameters vs. Frequency

A) Transition and Tapered Region

The tapered region was used for impedance matching from 50 ohm to a higher impedance. The sensing area was 13 mm by 24 mm rectangle filled with parallel directors. There is no ground plane from the backside.

B) Energy Transfer Region

As shown in the far field in Figure 2c, the proposed sensor was originally based on the idea of a dual-beam antenna published in [22], with perhaps an exception that each of the beams was formed by a periodic array of serially connected closed circular metal rings in the energy transfer region. The array was not a transverse transmission medium, with no ground plane underneath. Each of these periodic arrays of serially connected closed metal rings has its own resonant frequency given by $f_o = c/\left(2\pi r\sqrt{1+\varepsilon_r}\right)$, where c is the phase velocity of light, r is the average radius of the closed circular metal ring, ε_r is the permittivity of the FR4 substrate suspending the circuit [20, 21]. Based on the geometric details given in the original design in Fig. 1a, the resonant frequency should be at least 5 GHz. Since the glucose sensing operation occurred at 1.6-2.5 GHz frequency range, the array of the serially connected closed metal rings should be thought as a non-dispersive transmission medium with a broadband under-unity permeability [19]. When excited by a source of electromagnetic wave, each of the closed metal rings self-generated a close loop eddy current. By Ampere's law, each of eddy current loops should generate a magnetic field in opposition to the external magnetic field from its neighboring

ring, thereby producing a diamagnetic response with the effectively permeability falling below 1. The substrate material was FR4, which is a non-magnetic material. The loop eddy current in each of the metal rings is largely a conductive eddy current which is relatively less dependent of the substrate dielectric losses. Hence, the transmission line formed with serially connected closed-rings often exhibit a better performance in terms of loss reduction compared to split rings. Unlike those metamaterials based purely on split rings, the magnetic properties of the metamaterials based on closed metal rings are relatively less sensitive to minor positional errors or size disorders.

The diamagnetism of the arrays of closed rings does not violate the principle of causality because the phase velocity inside the arrays should remain less than the speed of light. This fact has been experimentally proven in [19] and [23].

C) Sensing Region

The sensing region was a region composed of metal grading densely spaced in sub-wavelength scale. The grating was arranged in the form of one-dimensional parallel wire array for y-polarized electric field plasma resonance, assuming that the y-direction is the direction of propagation. The spacing between each neighboring wires, a, is assumed to be very much less than the designated wavelength, i.e. C/2.7e9. The wire array was essentially a anisotropic dielectric medium with plasma resonance [13]. The two beams in Figure 2c has been largely polarized in majority to TM modes. As a result of this arrangement, the electric field passing onto the wires gave rise to a conductive current, yielding a strong response similar to a plasma.

At frequencies below the plasma frequency, ω_p, the axial component of the permittivity tensor of the sensing region essentially became negative. Let's assume that the two beams in Figure 2c were pointing to the x-direction. With this assumption, the effective permittivity of the sensing region can be expressed as a diagonal or near-diagonal tensor in the following manner:

$$\varepsilon_{eff} = \begin{bmatrix} \varepsilon_{xx} & 0 & 0 \\ 0 & \varepsilon_{yy} & 0 \\ 0 & 0 & \varepsilon_{zz} \end{bmatrix}$$

where ε_{yy} is the permittivity component parallel to the parallel wires. ε_{yy} is also frequency and spatially dispersive and can be negative, thereby allowing the sensing region to function as an artificial metamaterial. On the other hand, since ε_{xx} and ε_{zz} are the components perpendicular to the wires, they should be close to the permittivity of the background material.

Since the two beams as illustrated in Figure 2c were incident at a large angle relative to the normal of the parallel wires, a well known near-Littrow configuration has been formed. Under this condition, the diffracted electromagnetic waves were able to back-propagate almost along the incident paths, with the diffracted order coupling into the guided mode from the incident beams. In optics, this approach has been commonly used to achieve high sensitivity for sensing molecules of a low density [11].

During the process of glucose measurements, a glucose solution of approximately 1 micro-litre in volume was applied to the centre of the sensing region using a micro-pipette. The presence of

the glucose solution altered the dielectric properties of the sensing region, thereby perturbing the electromagnetic field interacting with the array of the parallel wires. As a result, a resonant frequency shift was observed at both of the resonances. The presence of the proposed near-Littrow configuration further reinforced the resonant effects.

D) Sensitivity Consideration

According to the simulated results in Figure 2d, the sensor should exhibit two resonances, with the primary resonance at around 2.42 GHz and the secondary resonance at around 1.54 GHz. The sensing region can be thought as a dielectric medium. In the absence of any glucose solution, the relative permittivity of the sensing region can be expressed using the Drude model as:

$$\varepsilon_{eff}=1+\frac{\omega_{p,m}^2}{\omega(1+j\gamma_m\omega)} \tag{1}$$

where $\omega_{p,m}$ is the plasma frequency of the parallel grating, γ_m is the damping factor of the metal in the parallel wire grating and ω is the operating frequency in radian. The plasma frequency of parallel grating without any dielectric substrate attached, $\omega_{p,m}$, can be approximately obtained with some modification to Pendry's formula using:

$$\omega_{p,m}=c\sqrt{\frac{1}{2\pi p\ ln\left(\frac{p}{kw}\right)}} \tag{2a}$$

where p is the grating period, w is the width of the wire and k is the adjustment factor that accounts for the rectangular cross-sectional area of each of the wire. The surface plasma frequency due to the grating/FR4 interface can be asymptotically obtained using

$$\omega_{sp}=\frac{\omega_{p,m}}{\sqrt{1+\varepsilon_{FR4}}}=\frac{c}{\sqrt{(1+\varepsilon_{FR4})\left(2\pi p\ ln\left(\frac{p}{kw}\right)\right)}} \tag{2b}$$

where ε_{FR4} is the relative permittivity of FR4. Because the metal thickness was 17 microns, the exact area of the wire cross-section was 1mm by 17 microns, which was $1.7\times10^{-8}\ m^2$. Using 1mm as the radius, the cross-sectional area would have been $7.8540\times10^{-7}m^2$. The adjustment factor k should be the ratio of these two figures combined, which should be 46.2. Substituting this adjustment factor to the expression given in equation (2b), we determined that the plasma frequency of the water without any glucose should be approximately 2.4956 GHz.

In the presence of the glucose solution, however, the overall permittivity can be expressed according to [14]:

$$\varepsilon_r=1+\omega_{sp}^2\sum_{j=0}^{M}\frac{S_j/S_0}{\omega_j^2-\omega^2-j\omega\gamma}+\frac{j\omega_{sp}^2}{\omega(\gamma_m-j\omega)} \tag{3}$$

where γ is the damping factor of the glucose solution itself. S_j is the oscillator strength, which is normally the number of free electrons per atom at jth resonance. The last term on the right side of Equation (3) is the conductivity according to Equation (1). The second term on the right side of Equation (3) is the harmonic model for non-conducting material, which, in this case, is the glucose solution. In Equation (3), it is assumed that the surface plasma frequency for the second term and the last term of the right side are the same. Let's assume that the metal used in the metal grating of the sensing region is perfectly conductive, which means $\gamma_m=0$. At frequencies very closed to a resonant frequency, ω_j, we have $\omega=\omega_j$. Equation (3) can be reduced to:

$$\varepsilon_r=1+\omega_{sp}^2\left(j\frac{S_j/S_0}{\omega_j\gamma}-\frac{1}{\omega_j^2}\right) \tag{4}$$

Differentiating Equation (4) with respect to ω_j, we get:

$$\frac{d\varepsilon_r}{d\omega_j}=\left(\frac{\omega_{sp}}{\omega_j}\right)^2\left(-j\frac{S_j/S_0}{\gamma}+\frac{2}{\omega_j}\right) \tag{5}$$

When the resonance is chosen to be at a microwave frequency, $2/\omega_j\approx 0$. Hence, Equation (5) can be further simplified to:

$$\frac{d\varepsilon_r}{d\omega_j}=\left(\frac{\omega_{sp}}{\omega_j}\right)^2\left(-j\frac{S_j/S_0}{\gamma}\right) \tag{6}$$

After some algebraic rearrangement, Equation (6) can be rewritten as:

$$\frac{d\varepsilon_r}{d\omega_j}=\frac{d(\varepsilon'+j\varepsilon'')}{dC}\frac{dC}{d\omega_j}=\left(\frac{\omega_{sp}}{\omega_j}\right)^2\left(-j\frac{S_j/S_0}{\gamma}\right) \tag{7}$$

where C is the concentration of the glucose solution on the surface of the sensing region. Under an anomalous dispersion, the sensitivity can be expressed as a change of resonant frequency per unit concentration, i.e. $\frac{d\omega_j}{dC}$. The sensitivity is always a real number. Therefore, the sensitivity can be readily obtained by separating the real part and the imaginary part from Equation (7).

By separating the real part and the imaginary part of Equation (7), and with some algebraic re-arrangement on Equation (7), the overall sensitivity of the sensing region becomes

$$\frac{d\omega_j}{dC}=\left(\frac{S_0}{S}\right)\gamma\left(\frac{\omega_j}{\omega_{sp}}\right)^2\frac{d}{dC}(\varepsilon'')$$

(8)

Where S, S_0, γ, ω_{sp}, C respectively stand for the oscillator strength at resonant frequency (ω_j), the oscillator strength at the highest resonance, the loss factor, the plasma frequency and the glucose concentration.

The sensitivity of a glucose sensing is undoubtedly an important figure of merit. While the near-Littrow configuration is important for achieving a high sensing sensitivity, it is also important to look at the other observations as revealed by Equation (8). These observations are summarized as follows:

I) In equation (8), the sensitivity is also proportional to the damping factor (γ) of the glucose solution or the substrate, meaning that the sensitivity is inversely proportional to Q-factor [12]. This Q-factor can be directly estimated by ratio of ($\frac{\omega_j}{\Delta\omega}$) over the frequencies in the neighborhood of the resonant frequency in the S11 plot.

II) Of these other factors, one of most obvious one was the plasma frequency or surface plasma frequency. Equation (8) suggests that the sensitivity is proportional to the square of $\left(\omega_j/\omega_{sp}\right)$. For achieving a higher sensitivity, the plasma frequency, ω_{sp} ,should be minimized, whilst the resonant frequency, ω_j, should be maximized. According to Equation (2b), the plasma frequency can be lowered by either increasing the periodical spacing between neighboring wires in the metal grating, p , or by decreasing the width of each of the metal strip in the sensing area. Since decreasing the metal strip in the sensing region is often associated with higher damping factor, the plasma frequency can be more cost-effectively lowered by increasing the spacing between each neighboring wires.

III) Equation (8) also reveals that not all the resonances are equal. The resonant frequency is always lower than or equal to the surface plasma frequency. Assuming that there exists more than one resonant frequency in the system, Equation (8) suggests that the resonances at lower frequencies tend to yield a lower sensing sensitivity.

E) Experimental Setup

Figure 3 shows the material resources used for our glucose measurements. Figure 3a shows the proposed sensor photolithographically fabricated in an FR4 substrate of 1mm thick. Figure 3b shows the glucose crystals as well as the weight scale that have been used for preparing the glucose solution.

Altogether, as shown in Figure 3d, we have prepared 9 sample solutions of different glucose concentrations. The lowest one was a pure water. During the measurement phase, each of the glucose sample solutions was applied to the sensing region using a micro-pipette as shown in Figure 3c. The volume of the liquid dispensable from the micro-pipette was adjusted to precisely 1 micro litre. All the chemicals and instruments used in this work are of clinical grade.

During the experiments, the measurements were cross-checked using a VNA and an experimental circuit as depicted in Figure 3e. As illustrated in Figure 3e, the experimental circuit has used a broadband hybrid directional coupler to separate the incident power, *a*, and the reflected power, *b*, associated with the glucose sensor. The signal source used in this work was ADF4351, which was equipped with a built-in low phase noise Voltage Control Oscillator (VCO) with the primary RF output frequency ranging from 2.2 GHz to 4.4 GHz and a built-in programmable frequency divider: 1/-2/-4/-8/-16/-32/-64. At each frequency within a permitted specific frequency range, ADF4351 generated a power of 4*a*. One-forth of the generated power from ADF4351 was expected to reach the glucose sensor, and another fixed portion of the same was delivered to the gain-phase detector as RFina. The AD8302 board was a gain-phase detector used to conduct analog computation of 10 $log_{10}(RFIna/RFInb)$ at each frequency within the designated frequency band. Figure 3f shows the experimental circuit wired according to Figure 3e.

(b) (c)

(d)

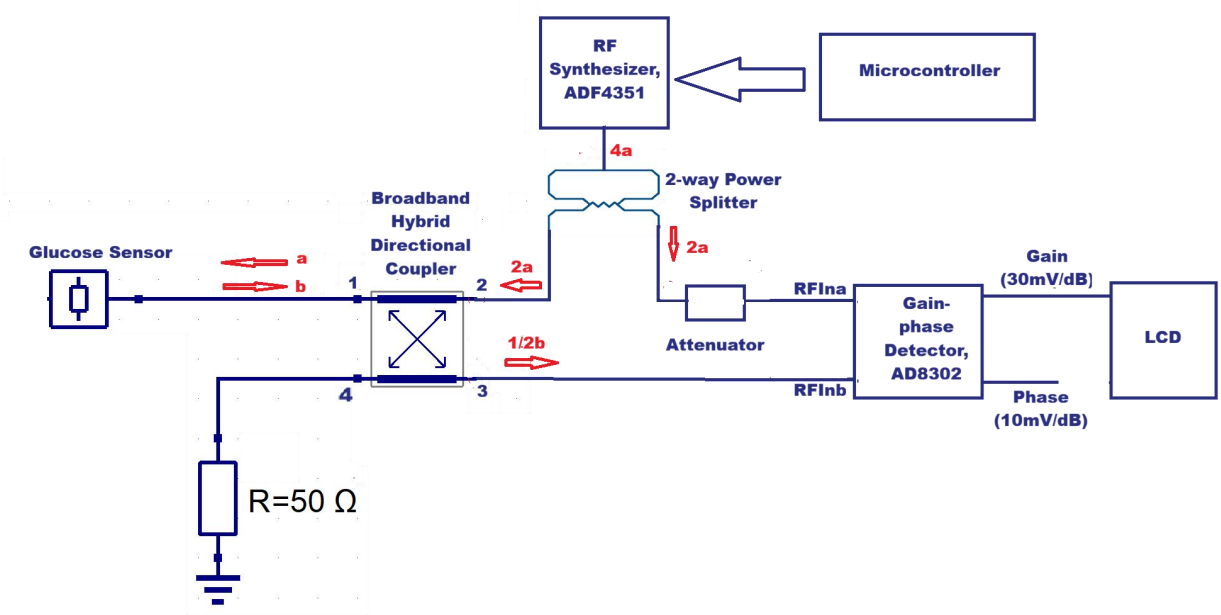
RF
Synthesizer,
ADF4351
Microcontroller
4a
2-way Power
Splitter
2a
Broadband
Hybrid
Directional
Coupler
Glucose Sensor
a
b
1
2
2a
RFIna
Gain
(30mV/dB)
Gain-
phase
Detector,
AD8302
LCD
Attenuator
1/2b
4
3
RFInb
Phase
(10mV/dB)
R=50 Ω

(e)

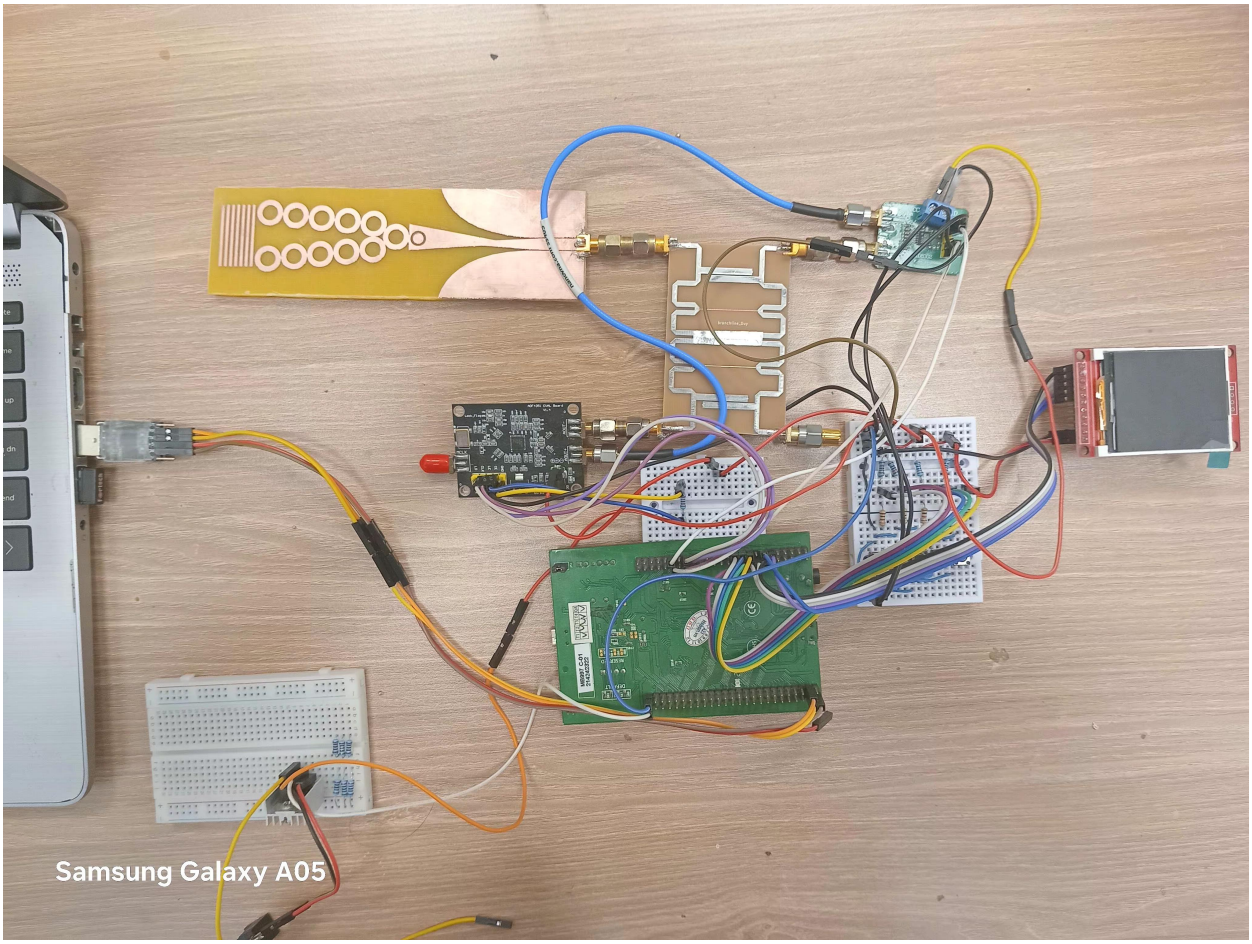

(f)

Figure 3. Experimentation Setup. (a) Proposed sensor fabricated in FR4; (b) Weight scale and glucose crystals used in the measurements; (c) Micro-pipette (d) Glucose samples; (e) Schematic diagram showing the measurement circuit involving AD8302; (f) Photo of the measurement circuit

III. Results and Discussion

Figure 4a shows the measured results of this work. In consistent with the simulated results depicted in Figure 2d, the measured results in Figure 4a have exhibited two resonant frequencies. The primary resonance has precisely occurred at around 2.42 GHz, as opposed to the value calculated using equation (2b) at 2.4956 GHz. As the simulation predicted, the secondary resonance has indeed occurred at around 1.54 GHz.

According to Figures 4b and 4c, all the sample concentrations have generated noticeable shifts in both of the resonant frequencies. More importantly, unlikely other published counter-parts, the

lowest glucose concentration that was noticeably detectable was found to be 25 mg/dL, thanks to the near-Littrow configuration in the sensing region of the proposed sensor.

A near-linear correlation between the glucose concentration and the resonance frequency was noticeably observed at both resonant frequencies, according to Figures 4d and 4e. In Figure 4d, it was observed the resonant frequency shift correlated with the glucose concentration almost linearly from 25 mg/dL up to 150 mg/dL. At 2.42 GHz, the range of this near-linear correlation between the resonant frequency and the glucose concentration has considerably exceeded the clinical diabetic range (see Figure 4d).

On the other hand, the resonant frequency shift at around 1.54 GHz did not correlate with the glucose concentration linearly. A near-linear correlation was moderately observable between 50 mg/dL and 125 mg/dL.

What is more important is the sensing sensitivity. This sensitivity can be obtained by calculating $\Delta f_o/\Delta C$, where f_o is the resonant frequency measured in GHz and C stands for the glucose concentration measured in mg/dL. The sensitivity can be readily estimated by measuring the maximum slopes of the graphs in Figures 4b and 4c. By estimation, the sensitivities specific to the resonances at 1.54 GHz and 2.42 GHz were respectively 800 kHz/(mg/dL) and 714 kHz/(mg/dL).

By direct observation on the graph in Figure 4a, the measured Q-factor at 1.54 GHz is lower. Consistent with our theoretical prediction, the measured sensitivity at 1.54 GHz was indeed higher for low glucose concentrations. In contrast with the measurements, however, the simulated Q-factor at 1.54 GHz turned out to be higher that of the resonance at around 2.42 GHz in CST simulation. This problem is very common in electromagnetic simulation. As yet, there has not been any conclusive resolution, although it has been suggested that eigenmode solvers often provids closer values to measurements compared to driven methods for high-Q structures [26].

However, as explained in the previous section, the sensitivity depends on not just the damping factor but also the ratio of (ω_j/ω_{sp}). It makes no sense to judge the sensitivity by looking at the Q-factor alone.

The return loss, which was also the S11 as measured in Figure 3a, was found to be lowest at 2.42 GHz. Contrary to a filter design, where lower return loss in the pass band is an indication of better performance, a higher S11 in a glucose sensing device is in most cases associated with a higher Q-factor. According to Equation (8), however, a lower Q-factor tends to yield a better sensitivity. In addition, not all the low return losses can be measurable by a gain-phase detector (e.g. AD8302) if the power reflected from a sensing device falls below -30dBm.

With the proposed measurement setup, most of the measurement processes were indeed automated with dramatic decrease in visualization errors which would otherwise be found with an vector network analyzer. However, the accuracy of the output display depends on the frequency resolution. During the verification stage, however, one of the major issues was the quantization noise contributed by the N-divider in the ADF4351 frequency synthesizer. We were

able to achieve around 7.8 kHz resolution, but not lower than this resolution. In ADF4351, the resolution is defined as PDF/MOD, where PDF stands for phase detection frequency and MOD stands for modulus. Unfortunately, the largest value of MOD that can be set in ADF4351 is 4095, which means that the minimum PDF that should be set is at least 10 MHz. With this in mind, another RF synthesizer with a better resolution should be used if higher resolution is required.

The proposed sensor employs dual resonances so that measurements can be independently cross-checked within a single experiment. Not only does this method ensure a greater accuracy and reliability, but it has been adopted in many applications. In standard electron density measurements, for example, a two-resonance probe is often used to measure electron density in low-pressure plasmas by simultaneously utilizing both plasma resonance and quarter-wavelength resonator resonance, with the results from these two types of resonances being compared for validation. In addition to the standard electron density measurements, there are many investigations that have successfully adopted dual mode measurement techniques [15-17]. In [17], for example, this technique has been very successfully used in a glucose sensing device, where the magnitude change and the resonance frequency shift were independently used to determine the concentration of a glucose-water solution, with an achievement of a higher accuracy and reliability within one single measurement. Another example was found in [16], where two light frequencies (pump and probe) were used to probe transitions between molecular energy levels, especially highly excited ones, often with sub-Doppler resolution, thereby facilitating assignment of quantum states and verification of theoretical models for applications like atmospheric studies. In [15], which is another example, the two excited modes were used to occupy the same volume of quartz, thereby allowing the resonator to sense two measurands simultaneously, with the end results proven to be more accurate.

(a)

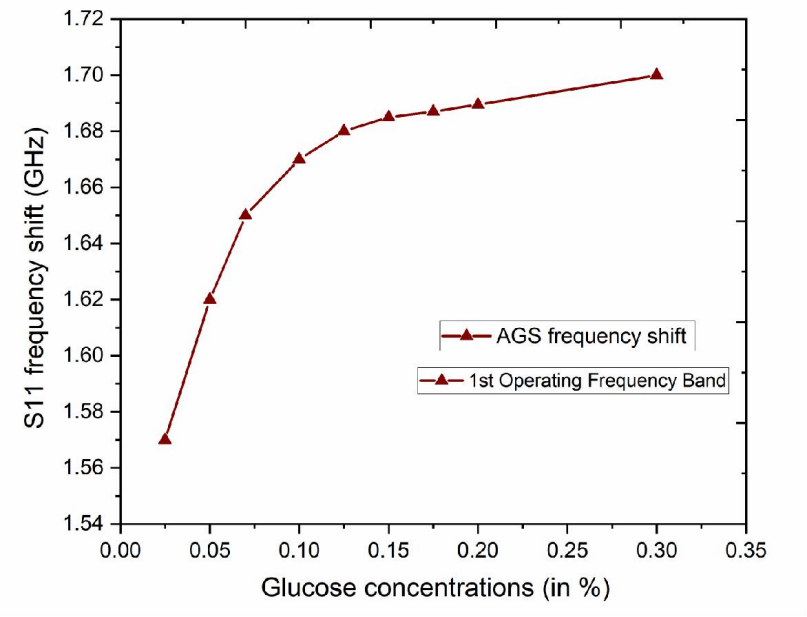

(b)

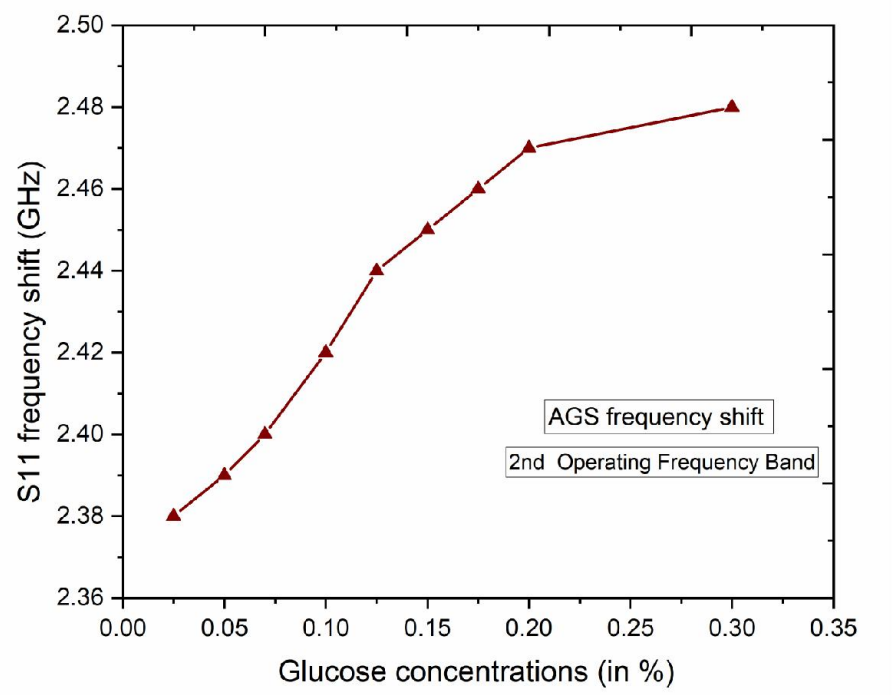

(c)

Figure 4. Measured Results. (a) Measured S-parameters; (b) A plot of resonant frequency against glucose concentration for the secondary resonance (i.e. at around 1.54 GHz); (c) A plot of resonant frequency against glucose concentration for the resonance at around 2.42 GHz; (d) Linear correlation between the resonant frequency and the glucose concentration for the resonance at around 1.54 GHz.

IV. Conclusions

In consistent with the simulated results, a sensing device with resonant frequencies below the threshold frequency of AD8302 has been successfully designed and realized on a lossy FR4 substrate, with one resonance occurring at around 2.42 GHz and the other occurring at arround 1.54 GHz. The realized sensor features the use of two closely packed periodic arrays of closed metal rings in the energy transfer region. A near-Littrow configuration has been successfully used in the sensing region for detection of ultra low concentration of glucose in a liquid solution, with the minimum detectable glucose concentration down to 25 mg/dL. The sensitivities that have been achieved were 715 kHz/(mg/dL) at the 2.42 GHz, and 805 kHz/(mg/dL) at 1.54 GHz. Dual resonances allow measurements of glucose concentration to be independently cross-checked and verified by providing two independent measurement frequencies within a single experiment, ensuring thereby greater accuracy and reliability.

Competing interests

The author(s) declare no competing interests.

Author Contributions

S.D: Conceptualization, Methodology, Simulations, Experiments, **L.WY.L:** Simulations, Data curation, Writing, **P.K:** Editing, Reviewing, Drafting, Supervision, **A.M.A:** Editing, Reviewing; **H.V:** Editing, Reviewing; **T.I:** Modeling, Editing, **E.G.A:** Project Administration, Writing, Review, Edit, **A.K:** Editing, Reviewing, Supervision.

Data availability statement

The datasets generated during and/or analysed during the current study are available from the corresponding author on reasonable request.

Funding:

This work is supported by Ongoing research funding program ORF-2026-482, King Saud University, Riyadh, Saudi Arabia and XJTLU research development funding project (RDF-24-02-004). This research is funded by the Vietnamese-German University under grant number DTCS2025-008.

References

[1] G. Gelao, R. Marani, V. Carrero and A. G. Perri, "Design of a Dielectric Spectroscopy Sensor for Continuous and Non-Invasive Blood Glucose Monitoring," International Journal of Advances in Engineering & Technology, vol. 3, no. 2, pp. 55-64, 2012.

[2] Mansour, E., Ahmed, M. I., Allam, A., Pokharel, R. K., & Abdel-Rahman, A. B. (2025). Sensitivity Evaluation of a Dual-Finger Metamaterial Biosensor for Non-Invasive Glycemia Tracking on Multiple Substrates. Sensors, 25(22), 7034.

[3] V. Pockevicius, V. Markevicius, M. Cepehas and D. Andriukaitis, "Blood Glucose Level Estimation Using Interdigital Electrodes," Elektronika ir Elektrotechnika, vol. 19, no. 6, 2013.

[4] Y. Liu, M. Xia, Z. Nie and J. Li, "In vivo wearable non-invasive glucose monitoring based on dielectric spectroscopy," in IEEE 13th International Conference on Signal Processing, 2016.

[5] Elsheakh DN, Mohamed E-H, Eldamak AR, "Blood Glucose Monitoring Biosensor Based on Multiband Split-Ring Resonator Monopole Antenna". Biosensors. 2025; 15(4):250. https://doi.org/10.3390/bios15040250

[6] Ja-Hao Chen and Keng-I Lai, "Cost-effective Noninvasive 2.4 GHz Microwave Blood Glucose Sensor", Sensors and Materials, Vol. 36, No. 5 (2024) 1905–1917, MYU Tokyo

[7] Danielle Nishida, "A Wearable 1.6GHz Non-invasive Midfield Wave-Based Blood Glucose Sensor", , California Polytechnic State University, San Luis Obispo, 2015.

[8] A. Kandwal et al., "A Novel Method of Using Bifilar Spiral Resonator for Designing Thin Robust Flexible Glucose Sensors," in IEEE Transactions on Instrumentation and Measurement, vol. 70, pp. 1-10, 2021, Art no. 8004810, doi: 10.1109/TIM.2021.3115201.

[9] Guodao Zhang, Qiwen Zhang, Chaochao Wang, Xiaojun Ji, Zhengqiu Weng, Abdulilah Mohammad Mayet, Xinjun Miao, A microstrip-based sensor for glucose monitoring: towards non-invasive blood glucose detection, Measurement, Volume 256, Part A, 2025, 118116, ISSN 0263-2241, https://doi.org/10.1016/j.measurement.2025.118116.

[10] Claire M. Watts, Xianliang Liu, Willie J. Padilla, "Metamaterial Electromagnetic Wave Absorbers", Advanced Materials, Volume 24, Issue 23, June 19, 2012.

[11] Nicolas Bonod and Jérôme Neauport, "Diffraction gratings: from principles to applications in high-intensity lasers", Advances in Optics and Photonics Vol. 8, Issue 1, pp. 156-199, 2016, doi: 10.1364/AOP.8.000156

[12] Kandwal, L. W. Liu, M. J. Deen, R. Jasrotia, B. K. Kanaujia and Z. Ni, "Electromagnetic Wave Sensors for Noninvasive Blood Glucose Monitoring: Review and Recent Developments", IEEE Transactions on Instrumentation and Measurement, vol. 72, pp. 1-15, 2023, Art no. 8007215, doi: 10.1109/TIM.2023.3327466.

[13] J. B. Pendry, A. J. Holden, W. Stewart, I. Youngs, “Extremely Low Frequency Plasmons in Metallic Mesostructures, Physical Review Letters 76, 4773 (1996).

[14] Baird, C. Lecture 2 Notes, Electromagnetic Theory II (University of Massachusetts, 2024).

[15] J. R. Vig, "Temperature-insensitive dual-mode resonant sensors - a review," in IEEE Sensors Journal, vol. 1, no. 1, pp. 62-68, June 2001, doi: 10.1109/JSEN.2001.923588.

[16] Foltynowicz A, et al, “Measurement and assignment of double-resonance transitions to the 8900-9100-cm-1 levels of methane”, Physical Review A, Volume 103, Issue 2, article id.022810.

[17] Abhishek Kandwal, Ziheng Ju, Louis W.Y. Liu, Rohit Jasrotia, Choon Kit Chan, Zedong Nie, Ali M. Almuhlafi, Hamsakutty Vettikalladi, “A dual-band microwave sensor for glucose measurements utilizing an enclosed split ring metamaterial-based array”, Engineering Science and Technology, an International Journal, 62, 101947, Feb 2025.

[18] NHS, BSol CGM Device Comparison Table, DMMAG for BSol IMOC. Version 1.2. Publication date: July 2024.

[19] H. S. Chen, L. Huang, and X. X. Cheng,”Magnetic Properties of Metamaterial Composed of Closed Rings”, Progress In Electromagnetics Research, Vol. 115, 317–326, 2011.

[20] M.B. Jasim and K.H. Sayidmarie, “Planar Absorbing FSS Unit Cells for Radar Cross-section Reduction”, IEEE 2022 International Conference on Innovation and Intelligence for Informatics, Computing, and Technologies (3ICT), Sakheer, Bahrain, pp. 476 – 480, 2022 (https://doi.org/10.1109/3ICT56508.2022.9990893).

[21] Basim, Mustafa & Sayidmarie, Khalil. (2023). Radar Cross-section Reduction of Planar Absorbers Using Resistive FSS Unit Cells. Journal of Telecommunications and Information Technology. 4. 61-67. 10.26636/jtit.2023.4.1331.

[22] Qi-Ye Wen, Yun-Song Xie, Huai-Wu Zhang, Qing-Hui Yang, Yuan-Xun Li, and Ying-Li Liu, "Transmission line model and fields analysis of metamaterial absorber in the terahertz band," Opt. Express 17, 20256-20265 (2009).

[23] Kandwal, A., Li, J., Igbe, T. et al. Broadband Frequency Scanning Spoof Surface Plasmon Polariton Design with Highly Confined Endfire Radiations. Sci Rep 10, 113 (2020). https://doi.org/10.1038/s41598-019-56720-4

[24] Louis W. Y. Liu, Abhishek Kandwal, Timo Oster, Klaus Hofmann, Choon Kit Chan, “Wireless Power Transfer by Spoof Surface Plasmon Polaritons at Ultrasonic Frequencies”, Progress In Electromagnetics Research M, Vol. 137, 79-86, 2026 doi:10.2528/PIERM25121707.

[25] Carlos Molero, Francisco Medina, RauĺRodríguez-Berral, and Francisco Mesa, "Making metals transparent: a circuit model approach," Opt. Express 24, 10265-10274 (2016)

[26] Grudiev A., Benchmarking HFSS and CST eigenmode and CST wake for waveguide damped cavities, [Lecture Notes] Retrieved on 11 May 2026. Retrieved from

https://indico.cern.ch/event/915543/contributions/3849520/attachments/2032841/3402733/20200506_IWG_slides_AG.pdf (2020).